
Effect of Blood-Brain Barrier Disruption on Intact and Fragmented Monoclonal Antibody Localization in Intracerebral Lung Carcinoma Xenografts

Edward A. Neuwelt, Peggy A. Barnett, Karl E. Hellström, Ingegerd Hellström, Christopher I. McCormick and Fred L. Ramsey

Oregon Health Sciences University, Portland, Oregon; Bristol-Myers Squibb, Seattle, Washington; and Oregon State University, Corvallis, Oregon

These studies highlight several factors that affect monoclonal antibody (Mab) localization to a tumor in the brain, including tumor permeability, nonspecific and specific binding, plasma half-life, radiolabeled antibody stability and the blood-brain barrier. **Methods:** A pancarcinoma Mab [L6 IgG, F(ab')₂ and Fab] and an irrelevant isotype-matched antibody [P1.17 IgG and F(ab')₂] were given with and without osmotic blood-brain barrier disruption in a LX-1 human small-cell lung carcinoma intracerebral xenograft model. **Results:** Intracerebral tumor size and permeability to antibody increased with the selection of 10, 14 or 17 days postinoculation when antibody was administered. Barrier disruption increased the delivery, particularly at earlier time points, which was dependent on antibody-specific and nonspecific binding and tumor permeability. Dehalogenation and/or antibody binding stability also appeared to affect the percent delivery. **Conclusion:** These studies demonstrate important variables that should be considered when clinical trials are designed or Mab delivery and localization in intracerebral tumor models are evaluated.

Key Words: blood-brain barrier; monoclonal antibody; xenografts

J Nucl Med 1994; 35:1831-1841

In initial clinical trials, localization of intact immunoglobulin (IgG) and Fab fragments to brain tumors (1-4) has been poor in the absence of any method to increase tumor permeability (0.0006%-0.0043% of the injected dose/g of tumor) (3). Delivery to tumors outside the central nervous system (CNS) has been higher (0.005% of the injected dose/g of tumor) (5). Houghton et al. (6) reported systemic tumor regression with a melanoma IgG₃ antibody concurrent with CNS progression. Some intracerebral human tumor xenografts in the nude rat (7) are significantly less

permeable to a variety of intravascular agents than are subcutaneous tumors in the same animal (8,9), but many of these intracerebral xenografts in animals are far more permeable to a variety of agents than are human brain tumors (3,12,11). The blood-tumor barrier, however, can be osmotically disrupted to increase drug delivery to a brain tumor (2,12-16). The concentration in the brain of small molecular weight markers, such as fluorescein and methotrexate (MTX), and high molecular weight markers, such as albumin, can be increased after osmotic blood-brain barrier disruption (BBBD) (8,17,18). Fab fragment delivery in human patients with CNS melanoma can be increased after BBBD, but persistent localization to the tumor has not been observed (19). It has been suggested by several investigators that methods or techniques that result in increased permeability in the intracranial tumor and surrounding tumor infiltrated normal brain may be required for effective therapeutic strategies that use monoclonal antibodies (Mabs) (4,20), and such was a major goal of this study. Previous studies evaluated tumor-specific IgM Mab delivery to the normal brain in rats and the effect of BBBD as a means to increase permeability to the antibody (21). The results showed a significant 20-fold increase in permeability to immunoreactive IgM Mab with BBBD but also demonstrated significant nonspecific binding that may greatly limit the use of IgM as a targeting agent in brain tumor therapy. This series of studies extends those observations to a brain tumor model and the evaluation of a tumor-specific Mab with more desirable properties.

Antibody delivery and localization with and without osmotic BBBD was sequentially evaluated using the pancarcinoma Mab L6 Fab, IgG and F(ab')₂ and an irrelevant isotype-matched IgG_{2a} Mab in LX-1 human small-cell lung cancer (SCLC) intracerebral xenografts. Because increasing tumor permeability was observed with increased tumor size, the authors also evaluated progressively smaller intracerebral xenografts at 17, 14 or 10 days postinoculation. The results suggest several factors that present problems in targeted delivery of an antibody to the CNS, in addition to

Received Dec. 22, 1993; revision accepted May 27, 1994.

For correspondence or reprints contact: Edward A. Neuwelt, MD, Oregon Health Sciences University, L603, 3181 SW Sam Jackson Park Road, Portland, OR 97201-3098.

TABLE 1
Selected Characteristics of the Monoclonal Antibody Studies

	Monoclonal antibody				
	L6 Fab (n = 34)	L6 IgG (n = 56)	P1.17 IgG (n = 31)	L6 F(ab') ₂ (n = 36)	P1.17 F(ab') ₂ (n = 42)
In vitro binding to LX-1 cells (%) [*]	9.8 ± 1.5	74.3 ± 2.9	14.9 ± 2.7	88.3 ± 1.8	7.3 ± 3.8
Specific activity (μCi/μg) [*]	6.87 ± 0.72	6.32 ± 0.82	10.27 ± 3.07	7.81 ± 1.34	8.81 ± 5.1
Weight loss (%) [†]	6.57 ± 1.52	6.06 ± 1.33	2.82 ± 1.51	1.42 ± 0.6	0.34 ± 0.67
Intracranial tumor weight (g) [*]	0.0739 ± 0.0146	0.0376 ± 0.0081	0.0384 ± 0.0138	0.0183 ± 0.0036	0.0184 ± 0.0048
Days postinoculation [†]	16.5 ± 0.6 (17-day model)	13.5 ± 0.5 (14-day model)	13.8 ± 0.3 (14-day model)	10.0 ± 0.1 (10-day model)	9.9 ± 0.1 (10-day model)
Half-life in plasma (hr)	11.5	30.4	41.4	15.9	63.8

^{*}Mean ± standard error of the mean.
[†]Mean ± 2 standard errors.
^{*}Median ± 2 standard errors.

the classic issues related to Mabs, such as tumor heterogeneity, antigen density and tissue clearance.

MATERIALS AND METHODS

Animal Tumor Model

Athymic nude rats from a colony maintained at the Oregon Health Sciences University were used for all experimental studies (8). Human SCLC LX-1 (22) were grown in culture (5% CO₂ at 37°C) in RPMI-1640 media with L-glutamine supplemented with 10% heat-inactivated fetal bovine serum, penicillin (10,000 units/ml), streptomycin (10,000 μg/ml) and gentamicin (50 μg/ml). Cultures of free-floating cell suspensions were harvested by centrifugation at 250 × g (1200 rpm) for 3–5 min. The cell pellet was resuspended in media to achieve a final packed cell volume of 20% ± 1% as measured in a microhematocrit tube. Cell viability was more than 85%, as determined by trypan blue exclusion. Inoculation of LX-1 tumor cells into the nude rats was stereotactically performed as previously described (8). In each animal, 10–12 μl (8–10 × 10⁵ cells) and 500 μl (4 × 10⁷ cells) of the prepared suspension was inoculated into the right hemisphere and subcutaneously into the right flank, respectively. The subcutaneous flank tumor was included in this model not only for the purpose of comparison with the intracranial tumor but also to provide a more clinically relevant model in which cranial metastases are usually present with extracranial lesions.

Monoclonal Antibodies

L6 is a mouse monoclonal IgG_{2a} antibody reactive with a propressophysin-like protein cell surface antigen abundant on human SCLC, breast carcinoma and colon carcinoma (23,24). P1.17, the nonspecific control antibody, is an IgG_{2a} mouse myeloma protein. These antibodies were provided by Bristol-Myers Squibb Pharmaceutical Research Institute (Seattle, WA). L6 and P1.17 Mabs have been well characterized both in vitro and in vivo by immunohistochemistry and Scatchard analysis. Membrane extracts from LX-1 cells and the propressophysin-like antigen extract have been studied by Western blot analysis (23–27). These studies have shown immunoreactivity of L6 IgG and L6 F(ab')₂ and the lack of immunoreactivity of P1.17. Fragments were prepared by papain digestion of the IgG, as previously described (19,28), but resulted in the loss of immunoreactivity of L6 Fab. Antibodies were labeled with ¹²⁵I by the chloramine-T method (19) and bound versus unreacted ¹²⁵I separated on a Sephadex G-25 M column (Pharma-

cia LKB, Biotechnology, Piscataway, NJ). After purification, protein binding of the radiolabel was determined by trichloroacetic acid (TCA) precipitation. Binding to LX-1 cells was periodically determined by an in vitro cell binding assay (13,29). The percent binding for the L6 IgG, L6 Fab, L6 F(ab')₂, P1.17 IgG and P1.17 F(ab')₂ were 74.3, 9.8, 88.3, 14.9 and 7.4, respectively (Table 1). The specific activity for L6 IgG, L6 Fab, L6 F(ab')₂, P1.17 IgG and P1.17 F(ab')₂ was 6.32, 6.87, 7.81, 10.27 and 8.81 μCi/μg, respectively. Preparations were stored at 4°C in 1% bovine serum albumin. Animals were given a dose of 18 to 19 × 10⁶ TCA-precipitable cpm (0.76–1.23 μg), measured just prior to each animal experiment.

Localization Experiments

These studies were performed in three phases in which Fab, IgG or F(ab')₂ was evaluated. Animals were anesthetized with sodium pentobarbital (50 mg/kg intraperitoneally), and BBBB in the rat was performed as previously described (30). Experimental groups were established in which L6 or P1.17 IgG or their fragments were administered as an intracarotid bolus immediately after intracarotid normal saline (control) or intracarotid 25% mannitol (BBBD) 10–17 days postinoculation. Because L6 Fab did not localize to the LX-1 tumor, further control studies with P1.17 Fab were not performed. To simulate the clinical situation better relative to tumor permeability, progressively smaller tumors were used (Table 1). Prior to the saline or mannitol infusion, Evans blue (2%, 0.5 ml) and fluorescein (10%, 0.12 ml) were administered intravenously. The mortality rate in this study was approximately 15%; two-thirds of the deaths occurred in mannitol-infused animals and one-third in normal saline control animals. The mortality rate was equal among males and females. Ninety percent of all deaths occurred in the 24-hr and 72-hr studies, presumably from complications of anesthetic recovery in animals with symptomatic brain tumors. For at least 4 days prior to the study, the animals received potassium iodine in their drinking water to block thyroid uptake of the radioactive iodide (21).

After saline or mannitol and Mab infusion, the animals were killed at 0.5, 3, 24 or 72 hr. A plasma sample was obtained before whole-body perfusion, which consisted of an intravenous infusion of 40–60 ml of normal saline warmed to 37°C with concurrent withdrawal from the intracarotid catheter until the heart stopped (30). This perfusion technique resulted in greater than 95% elimination of the intravascular radioactivity. With clean gloves, the brain (lowest count tissue) was removed first and Evans blue staining was mac-

roscopically graded as previously described (30) followed by removal of the subcutaneous tumor (SQT). Prior experience with nonperfused animals showed this technique does not result in radioactive contamination from blood. Samples were then rapidly frozen (-80°C) for at least 24 hr prior to regional sampling.

Statistical Analysis

The results are expressed as the percentage of the total TCA-precipitable injected dose (TD) per gram of tissue. The effect of disruption was evaluated in integrated periods of (1) 0–0.5 hr, (2) 0–3 hr, (3) 0–24 hr and (4) 0–72 hr after saline or mannitol infusion and Mab administration. The percent difference (R) in the area under the curve (AUC) was calculated for each integrated period as follows:

$$R = \frac{100 (\text{AUC after mannitol} - \text{AUC after saline})}{\text{AUC after saline}}$$

The localization index for L6 IgG and L6 F(ab')₂ was calculated in nondisrupted animals with the AUC for the 72-hr experimental period as follows:

Localization index

$$= \frac{\text{Mean AUC for specific (Mab in tissue)/(Mab in plasma)}}{\text{Mean AUC for nonspecific (Mab in tissue)/(Mab in plasma)}}$$

The data were analyzed as three separate experiments (Fab, IgG or F(ab')₂) with multivariate analysis of covariance (31) in which the principal response variable was Mab concentrations in tissues. The design factors were (1) antibody L6 or P1.17, (2) time of sacrifice at 0.5, 3, 24 or 72 hr after treatment and (3) saline or mannitol treatment. The covariables evaluated were sex, days postinoculation when Mab was given and animal weight at inoculation. The preliminary analysis showed systematic differences in variance of all responses except weight loss. Homogeneity of variation was obtained by a transformation of the responses to a logarithmic scale. To estimate half-lives, exponential lifetime distributions in the plasma were assumed.

The analysis of covariate effects within each of the three major studies (Fab, IgG and F(ab')₂) was measured by a step-up variable selection procedure with the multivariate likelihood ratio test statistic. The percent weight loss of animals was the most significant covariate ($p = 0.003$, $p = 0.018$, $p = 0.0001$). Higher weight losses were associated with higher concentrations in the plasma. The animal's weight at inoculation had a significant effect in the IgG and F(ab')₂ studies ($p = 0.0001$ and $p = 0.004$, respectively) but not in the Fab study ($p = 0.81$) in which heavier animals had generally lower concentrations in the contralateral left hemisphere, subcutaneous tumor and plasma. Within each of the three studies, intracerebral tumor weight had no strongly significant overall associations with tissue concentrations, and no statistical association was found between sex and concentrations. Although it was believed that days postinoculation had a strong influence on the different results between the three different studies, there was little variation within a study, and these variations had no significant associations with tissue concentrations ($p = 0.19$ [Fab], $p = 0.63$ [IgG] and $p = 0.065$ F(ab')₂).

Figures and discussions are based on the concentrations adjusted within each study for differences in all covariates. The unadjusted raw data (in counts per minute per gram or milliliter), expressed as the mean \pm standard error of the mean (s.e.m.), for

each treatment group in selected tissues and plasma are also presented in Table 2.

RESULTS

LX-1 Tumor Model

A typical coronal section from an LX-1 intracerebral tumor-bearing nude rat at 14 days postinoculation is shown in Figure 1A. These tumors were generally well demarcated and occasionally contained multiple lobes or demonstrated some ventricular seeding. In this model, the median survival was approximately 20 days. Quantitative whole-body autoradiography demonstrated excellent localization of L6 IgG to intracerebral and subcutaneous LX-1 tumors 72 hr after administration (Fig. 1B). The autoradiography was performed by Dr. Irwin Fand (32). Periodic immunohistochemical evaluation with L6 IgG and L6 F(ab')₂ consistently showed excellent binding to tumor cell surface antigens (26). In vitro cell binding assays were regularly performed throughout this study and continuously demonstrated a high percentage binding for L6 IgG and L6 F(ab')₂. Specific Mab binding ranged from 74% to 88%, and nonspecific binding ranged from 7% to 15% (Table 1).

Intravascular Radioactivity Clearance

The saline perfusion technique used to remove intravascular radioactivity effectively removed $96.63\% \pm 0.28\%$ (mean \pm s.e.m. of all treatment groups) from the vascular compartment (Table 2). Separate studies in this model that used a poorly penetrating macromolecule (dextran, molecular weight 70,000) after 10 min following intracarotid bolus administration determined the intravascular volume at 8–16 days postinoculation of tumor cells (manuscript in preparation). When the approximate plasma volume for each tissue was known, the influence of remaining plasma radioactivity on tissue levels was evaluated. Intravascular volume for the Fab, F(ab')₂ and IgG studies, respectively, were 0.0493, 0.0225 and 0.0359 ml/g in intracranial tumor (ICT), 0.0289, 0.0209 and 0.0294 ml/g in normal brain distant to tumor (BDT) and 0.0254, 0.0352 and 0.0303 ml/g in SQT.

From the treatment group mean values in the ICT and SQT groups shown in Table 2, there was only one instance in which the intravascular concentration after perfusion contributed more than 10% of the tumor radioactivity (14.2% in ICT in Group 17). There were an additional seven instances in which tumor radioactivity was influenced by postperfusion plasma radioactivity by 5%–10%. In all eight instances, this occurred at 0.5 hr after administration when the preperfusion and postperfusion plasma concentrations were the highest and the tissue concentration was the lowest. In most tumor samples, the effect of the plasma concentration was less than 2%.

In the BDT, the contribution of the remaining plasma radioactivity was less than 2% in the BBB groups (Table 2). However, in the normal saline groups in which the BDT concentration was extremely low (less than 0.02% of the administered dose), there was a significantly higher contri-

TABLE 2
Raw Unadjusted Data (in Counts per Minute per Gram or Milliliter) After Monoclonal Antibody Administration with or without Blood-Brain Barrier Disruption in LX-1 SCLC Xenografts*

Group	TXT	Time	Agent	No.	ICT		BDT		SQT		Preperfusion plasma		Postperfusion plasma	
					Mean	s.e.m.	Mean	s.e.m.	Mean	s.e.m.	Mean	s.e.m.	Mean	s.e.m.
1	NS	0.5	L6 Fab	5	25,295	10,373	1997	685	21,480	3931	490,559	54,404	19,995	7988
2	NS	3	L6 Fab	5	25,441	7943	5227	3505	44,646	19,643	240,551	83,677	5081	2408
3	NS	24	L6 Fab	3	25,821	11,363	1651	821	41,815	22,642	31,041	3004	1583	617
4	NS	72	L6 Fab	3	3561	1460	247	89	15,904	1268	7340	1734	454	224
5	BBBD	0.5	L6 Fab	5	83,068	38,040	90,236	31,495	32,528	10,471	857,052	95,050	24,328	4195
6	BBBD	3	L6 Fab	5	98,634	28,357	70,662	31,366	33,188	4505	173,251	36,857	8721	2433
7	BBBD	24	L6 Fab	4	24,495	5145	15,342	4995	21,928	5280	26,344	10,232	1444	541
8	BBBD	72	L6 Fab	4	3430	593	944	489	14,225	3476	2974	518	87	17
9	NS	0.5	L6 F(ab') ₂	4	23,275	3033	1799	468	15,048	1651	1,652,652	48,180	41,115	12,357
10	NS	3	L6 F(ab') ₂	5	37,024	5788	1625	335	37,921	5829	918,069	101,239	26,434	6887
11	NS	24	L6 F(ab') ₂	4	26,394	5374	514	112	29,055	3380	22,708	3104	1285	324
12	NS	72	L6 F(ab') ₂	4	5572	2227	79	23	14,049	3144	2050	501	42	8
13	BBBD	0.5	L6 F(ab') ₂	5	51,373	13,300	98,749	18,784	20,075	3944	1,557,573	72,363	19,784	2433
14	BBBD	3	L6 F(ab') ₂	4	87,759	12,031	156,077	25,853	30,052	403	866,052	116,083	18,067	7682
15	BBBD	24	L6 F(ab') ₂	4	69,513	10,246	36,206	11,045	41,335	5376	38,811	12,481	1227	477
16	BBBD	72	L6 F(ab') ₂	4	16,697	6827	12,802	6770	11,768	3325	2536	554	79	21
17	NS	0.5	P1.17	5	7030	2042	1596	220	19,322	2258	1,437,196	72,717	44,440	11,303
18	NS	3	P1.17	5	37,131	6846	1715	287	41,819	6226	713,409	65,851	17,001	4192
19	NS	24	P1.17	4	23,379	5938	717	169	24,481	4044	115,255	33,522	2869	401
20	NS	72	P1.17	6	3731	918	654	230	3568	920	6264	1897	318	149
21	BBBD	0.5	P1.17	4	49,424	21,498	122,670	47,688	22,504	2430	1,389,181	48,460	36,690	7779
22	BBBD	3	P1.17	5	117,460	60,857	138,447	16,842	60,319	15,964	795,455	40,220	17,267	2747
23	BBBD	24	P1.17	4	56,464	16,163	84,693	29,193	16,745	2363	72,279	17,242	1674	232
24	BBBD	72	P1.17	4	7469	1813	11,504	3921	6002	2363	6210	594	665	248
25	NS	0.5	L6 IgG	10	24,463	4211	5363	1762	20,810	1952	1,965,644	147,417	53,970	13,759
26	NS	3	L6 IgG	8	78,996	22,306	2335	486	65,350	10,587	1,611,732	177,079	44,197	9600
27	NS	24	L6 IgG	6	211,356	35,948	7338	3642	258,470	51,689	616,830	68,103	37,893	10,740
28	NS	72	L6 IgG	6	228,547	38,689	6770	3857	370,166	41,054	363,851	49,937	9976	2917
29	BBBD	0.5	L6 IgG	11	65,575	12,037	91,443	15,736	30,547	5901	1,886,560	112,763	35,485	8154
30	BBBD	3	L6 IgG	7	107,017	22,172	106,524	19,925	94,186	29,172	1,496,964	118,389	23,653	6762
31	BBBD	24	L6 IgG	6	173,960	21,244	98,568	26,531	159,699	18,998	672,901	94,907	33,041	6941
32	BBBD	72	L6 IgG	6	156,933	35,342	17,429	3710	391,328	47,020	389,240	39,702	13,121	5706
33	NS	0.5	P1.17 IgG	3	18,822	1109	1124	221	15,684	2073	1,958,655	241,982	32,585	5600
34	NS	3	P1.17 IgG	4	33,874	5266	1744	445	55,850	9088	1,456,715	115,549	38,097	4704
35	NS	24	P1.17 IgG	4	72,478	9175	2639	480	107,858	21,249	642,060	109,468	28,417	5497
36	NS	72	P1.17 IgG	4	67,677	7088	35,440	17,355	117,816	32,036	547,614	22,999	16,907	7151
37	BBBD	0.5	P1.17 IgG	4	40,551	7315	161,980	44,347	29,978	7049	1,628,119	244,853	26,012	11,556
38	BBBD	3	P1.17 IgG	4	40,773	3161	59,152	5500	39,647	6293	1,464,284	108,343	34,431	6356
39	BBBD	24	P1.17 IgG	4	93,594	7500	48,838	17,134	81,313	10,699	545,525	57,619	19,979	5297
40	BBBD	72	P1.17 IgG	4	63,315	5135	30,723	17,428	107,056	29,743	419,547	66,028	8877	3596

*Monoclonal antibodies L6 Fab, F(ab')₁, or IgG and P1.17 F(ab')₂ or IgG (18–19 × 10⁶ cpm) were given by intracarotid injection after NS or mannitol (BBBD) infusion. Animals were killed by saline perfusion at 0.5, 3, 24 or 72 hr after Mab administration.

ICT = intracranial tumor; BDT = normal brain distant to tumor; SQT = subcutaneous tumor; TXT = treatment; NS = normal saline; BBBD = blood-brain barrier disruption; s.e.m. = standard error of the mean.

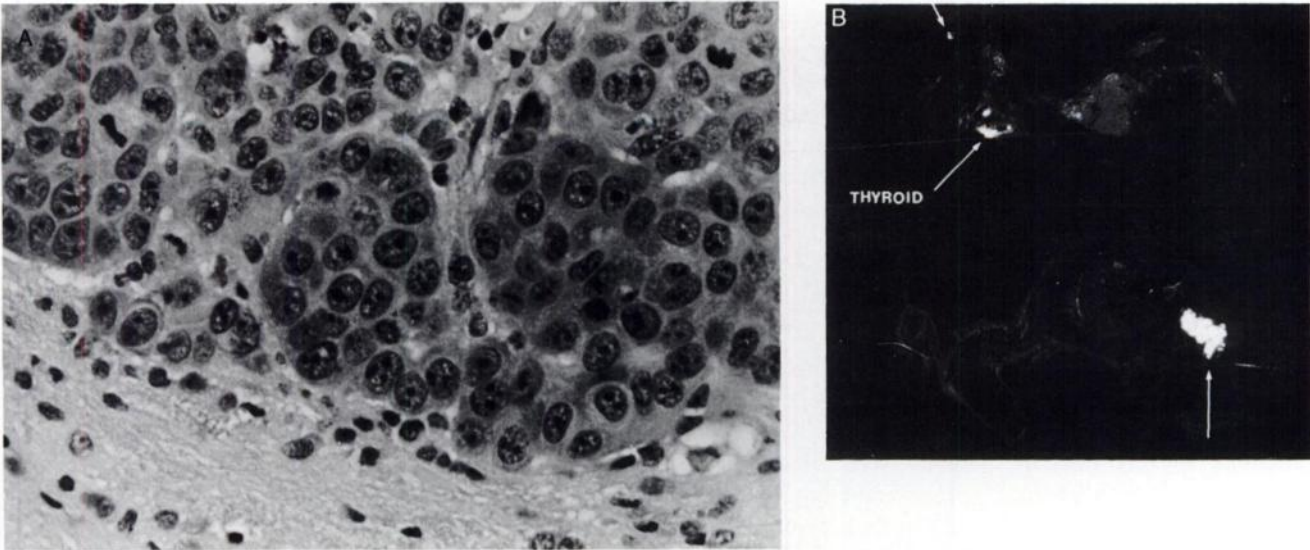


FIGURE 1. (A) Brain: tumor interface of a typical LX-1 small-cell lung carcinoma xenograft in a nude rat 14 days after inoculation with LX-1 cells (H & E 400 X). (B) Whole-body autoradiogram of an LX-1 SCLC intracerebral and subcutaneous tumor-bearing nude rat 72 hr after intracarotid saline (nondisrupted) and iodinated L6 IgG administration (0.75 μ Ci/g body weight) (Courtesy of Dr. Irwin Fand).

bution from the plasma (20%–85%), particularly at the earlier time points.

Fab Fragment Studies

Based on studies in normal nontumor-bearing rats, it was initially thought that the Fab fragment was likely to have the most desirable pharmacokinetic characteristics, i.e., rapid plasma clearance and the rapid clearance from

nontumor-infiltrated brain because of the absence of the Fc portion of the Fab fragment (30,33). However, the L6 Fab fragment served as a control Ig in terms of tumor specificity because the immunoreactivity was lost during preparation. In the current studies, the plasma half-life was 11.5 hr. As illustrated in Figure 2, compared with the saline control, there was a significant increase in the concentration of L6 Fab in ICT after BBBD over the initial 24 hr of observation

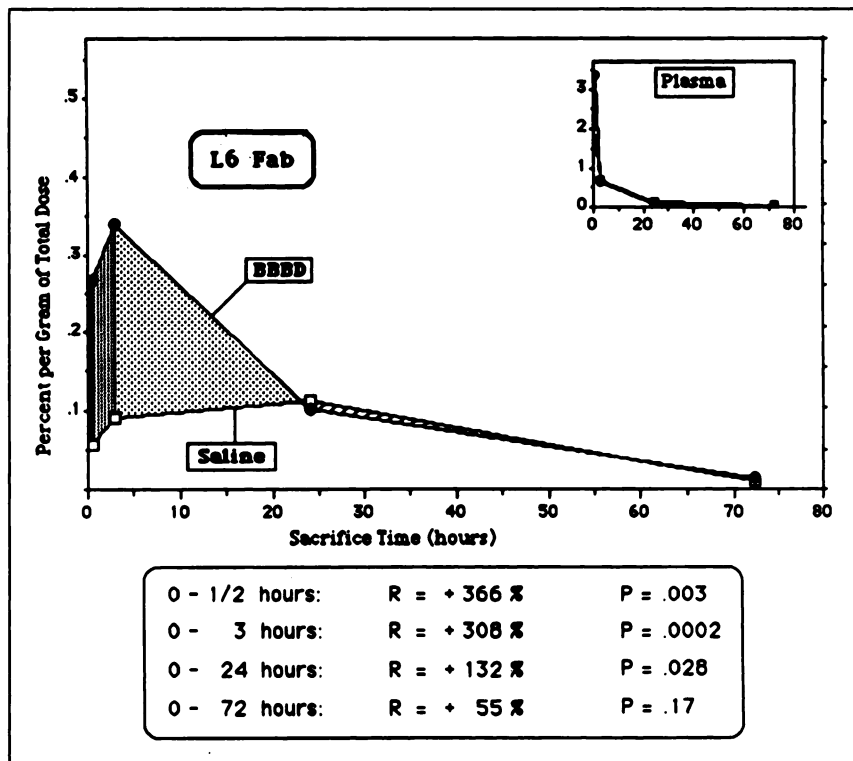


FIGURE 2. Concentration (percent of total dose/g tissue) in intracranial tumor following intra-arterial administration of 125 I-labeled L6 Fab after mannitol (BBBD) or saline as compared with intervals over time (0–72 hr). R = percent difference in the area under the curve for each integrated period.

(0.35% of the injected dose at 3 hr). The increase was particularly marked during the initial 3 hr in which the AUC increased by 308% ($p = 0.0002$). The plasma curves were virtually superimposable, which indicated that plasma concentration was not responsible for this increase (Fig. 2). Most of the L6 Fab was cleared from the tumor and normal brain rapidly within 24 hr after administration. In the absence of disruption, less than 0.1% of the injected dose was measured in ICT.

The L6 Fab study was performed in animals with relatively large ICTs with a median weight of 0.0739 ± 0.0146 g (Table 1). The average weight loss at the time of sacrifice was $6.57\% \pm 1.52\%$ of their total body weight. This occurred at an average time of 16.5 days after ICT cell inoculation. At this time, the animals were preterminal and symptomatic, as evidenced by the weight loss. The lack of antigen binding with the L6 Fab (Table 1) resulted in transient delivery of the Fab fragment to both the ICT and SQT.

IgG Studies

In the second phase of this study, intact IgG was evaluated. The *in vitro* binding to LX-1 tumor cells was 74.3% for the L6 IgG in contrast to 14.9% for the irrelevant antibody P1.17 (Table 1). In the IgG studies, Mabs were administered at an earlier time point (average 13.6 days) in which the animals were less symptomatic. The resulting tumors were approximately half as large as in the first phase of the study (average 0.0379 g). The plasma half-life was three to four times longer for IgG compared with Fab. There was an increase in antibody delivery after BBBD but only during the initial 3 hr of study with L6 IgG (Fig. 3A) and over the entire 72-hr experimental period with P1.17 IgG (Fig. 3B). There was greater and more persistent localization to both ICT and SQT with the L6 IgG compared with the irrelevant P1.17 antibody, as illustrated in Figure 4. After BBBD, the concentration of L6 IgG and P1.17 IgG remained in both the brain around the tumor (BAT) and normal brain. The localization index in the absence of BBBD for L6 IgG in ICT was 3.29 ± 0.79 , 3.38 ± 0.68 in SQT and 0.36 ± 0.15 in BDT.

An additional study was performed to evaluate intact IgG delivery at an earlier time postinoculation (10 versus 14 days) when the ICT may be even less permeable and, thereby, more relevant to the clinical situation (34,35). Tumor permeability to L6 IgG measured 72 hr postadministration, in the absence of disruption, was decreased at 10 days postinoculation, as evidenced by antibody levels of $0.350\% \pm 0.163\%$ of TD ($n = 4$) compared with levels at 14 days postinoculation of $1.238\% \pm 0.192\%$ TD ($n = 6$, $p = 0.04$). In addition, the mean ICT weight was much less in the 10-day postinoculation group (0.0111 versus 0.0400 g).

F(ab')₂ Studies

Based on these results, L6 F(ab')₂ was evaluated in the smaller, less permeable 10-day postinoculation model. The *in vitro* cell binding for L6 F(ab')₂ was 88.3%. The concentration of the F(ab')₂ in ICT again showed a significant

increase after BBBD compared with that in the nondisrupted control animals over the 72-hr experimental period (Fig. 5). The concentration in BAT and normal brain were also significantly increased after BBBD followed by rapid clearance. In the absence of disruption, 0.1% TD and 0.2% TD of P1.17 F(ab')₂ and L6 F(ab')₂, respectively, were measured in ICT. For unclear reasons, the plasma half-life is significantly different for the L6 (15.9 hr) and P1.17 (63.8 hr) F(ab')₂ (Fig. 5). The localization index, which controls for plasma differences, of L6 F(ab')₂ was 3.80 ± 1.00 in ICT, 5.29 ± 0.96 in SQT and 1.15 ± 0.28 in BDT.

Although the L6 F(ab')₂ *in vitro* cell-binding capacity (88.3%) was higher than intact IgG (74.3%), concentration of L6 F(ab')₂ in ICT or SQT was much lower and did not persist compared with intact IgG (Fig. 4). There are two possible explanations for the lower measured L6 F(ab')₂ concentrations. The F(ab')₂ fragment may not be as stable *in vivo* and, thereby, have decreased antigen binding capacity and be cleared rapidly from the tumor. Another possibility is more rapid dehalogenation of F(ab')₂. A preliminary study with the L6 and P1.17 IgG and F(ab')₂ showed a three- to fivefold greater accumulation of radioiodine in the thyroid after F(ab')₂ administration, suggesting accelerated dehalogenation. There was also no difference in delivery of L6 F(ab')₂ to tumor, whether iodinated by the chloramine-T or iodogen methods. Thus, it appears that F(ab')₂, whether intact or degraded, is dehalogenated much more rapidly than IgG.

DISCUSSION

Factors that Influence Mab Delivery to Brain Tumors

Tumor Permeability. Several factors influence Mab delivery to experimental brain tumors (11,32,36-44). The largest variable is the permeability of the animal tumor model. Permeability measurements vary widely among and within animal tumor models. However, nearly one-third of human malignant gliomas have an intact BBB to contrast agents, and virtually all malignant gliomas and probably most brain metastases have areas of tumor with an intact BBB (45-48). Although therapeutic efficacy can be demonstrated with radiolabeled antibody in experimental brain tumor models (20,49), such models are often much more permeable than human tumors and thus may not relate to clinical circumstances (3,11). For instance, a number of studies have been reported in the D54 human glioma xenograft model. However, the permeability of this intracerebral xenograft is one of the highest in the reported literature, and brain tumor levels of irrelevant antibody are in the same range as in an SQT or in other organs that do not have a BBB (10,34).

The current studies were performed at three different time points after tumor cell inoculation. The ICTs in the L6 Fab studies, at 17 days postinoculation, were very large, vividly stained with Evans blue albumin, as in the SQTs, and the animals were at the end stage of disease progression. This tumor did not seem clinically valid in a study that

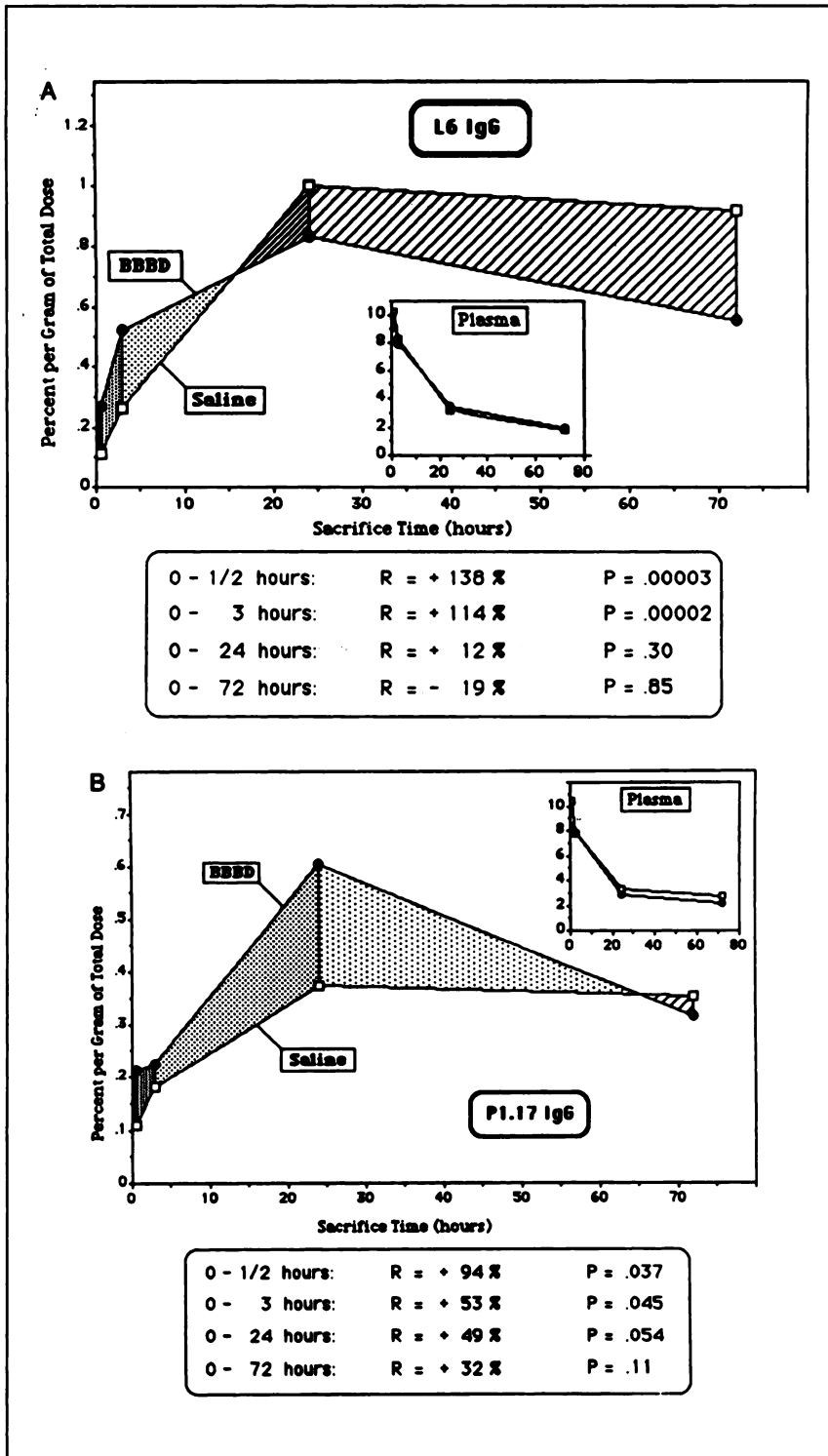


FIGURE 3. (A) Concentration (percent of total dose/g tissue) in intracranial tumor following intra-arterial administration of ^{125}I -labeled L6 IgG after mannitol (BBBD) or saline as compared to intervals over time (0-72 hr). (B) Concentration (percent of total dose/g tissue) in intracranial tumor following intra-arterial administration of ^{125}I -labeled P1.17 IgG after mannitol (BBBD) or saline as compared with intervals over time (0-72 hr). R = percent difference in the area under the curve for each integrated period.

evaluated a method for increasing tumor permeability to large molecular weight antibodies. Thus, the IgG studies were evaluated in the 14-day model in which the tumors were smaller and the animals less symptomatic. Tumor size has been reported to affect both permeability and antibody uptake (11,20,50). However, as reported in these results, the ICT in the 14-day model still was relatively permeable and allowed three to four times more delivery of

L6 IgG compared with concentrations at 10 days postinoculation. Thus, the last series of studies with F(ab')_2 were performed at 10 days postinoculation.

Specific and Nonspecific Binding. Tumor cell binding capacity of the antibody has obvious importance. Except for the L6 Fab studies, this does not appear to be a major issue with L6. The affinity of the L6 antibody is certainly acceptable (3×10^8) (24), and the localization to the SQT,

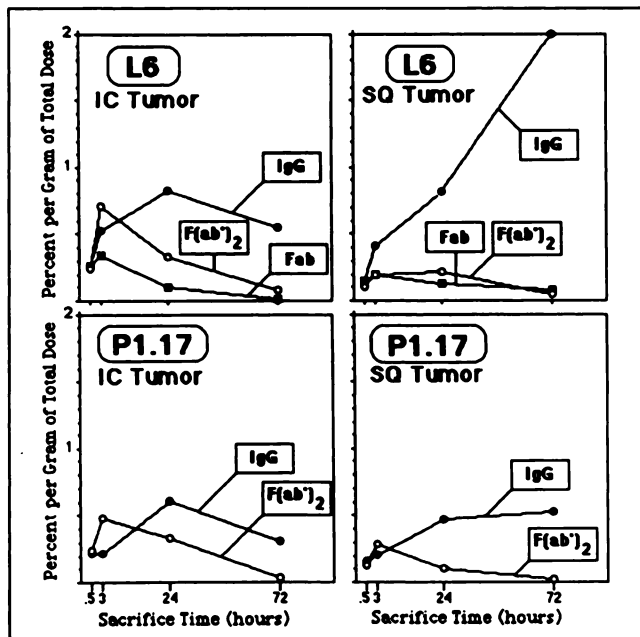


FIGURE 4. Concentration (percent of total dose/g tissue) over time comparing L6 IgG, Fab, and F(ab')₂ to P1.17 IgG and F(ab')₂ localization in intracranial and subcutaneous tumor after osmotic BBBB.

in which the barrier is not a factor, was far from the maximum even at 72 hr. In addition, the in vitro binding was higher than that reported for many antibodies (3). The explanation for the lower localization of L6 compared with that in the literature may be the result of the use of a less permeable brain tumor model.

The presence or absence of the Fc portion on the antibody and the rate of clearance of Mab from plasma and normal tissue has also been evaluated (4,30,33,38,51). In the reports by Colapinto et al. of localization (38) and therapy (51) in the D54 human glioma model that used IgG Mel-14, the percent of injected dose per gram of tissue was approximately 2% for both the specific and nonspecific antibody at 40 min. At 48 hr, the percent of the dose per gram of tumor rose to nearly 16% with the specific antibody but remained at 4% with the isotype-matched irrelevant antibody. This is an example of both nonspecific and specific binding of intact antibodies (10,38). Colapinto et al. (38) also demonstrated higher tumor-to-normal tissue ratios of the F(ab')₂ fragment compared with intact IgG, but studies have consistently reported lower concentration of fragments localized to tumor compared with IgG (38,52,53). The L6 IgG localization to the tumor was higher than both P1.17 IgG or L6 F(ab')₂. There can be a decrease in binding affinity inherent in the generation of fragments, and loss of immunoreactivity was the case with L6 Fab where in vitro binding was less than 10%.

A major problem that complicates the interpretation of the F(ab')₂ studies appears to be dehalogenation and/or a faster catabolism throughout the body; this results in the liberation of radioiodine. The stability of the radiolabeled antibody is

not a new issue and appears to be a significant problem, particularly in these L6 F(ab')₂ studies (54,55). Zalutsky et al. (54,55) examined the issues of halogen labeling in detail. Thyroid uptake is proportional to the rate of dehalogenation (55), and a preliminary study demonstrated dehalogenation for L6 and P1.17 F(ab')₂ was fourfold faster than for IgG. Additional experiments in which more stable labels are used and immunologic studies of Mab degradation will be required to help determine the mechanisms of dehalogenation. In vivo antibody extraction studies in which immunoreactivity is evaluated will be necessary to determine if there is also in vivo binding instability (21).

The localization index was calculated from concentrations over the 72-hr experimental period in control nondisrupted animals. The localization index for L6 IgG in ICT was in the same range as that reported for Mel-14 IgG and 81C6 IgG (38,54,56). However, the localization index for L6 F(ab')₂ was much lower than that reported for Mel-14 F(ab')₂, probably because a less permeable tumor model was used and the effects of dehalogenation were a factor.

Delivery and Localization of Fab, IgG and F(ab')₂ L6 Fab behaved in a manner most analogous to a standard drug, such as MTX, in that it had a relatively short plasma half-life and no biologic specificity. Delivery to ICT was also increased after BBBB. In addition, similar to most drugs, Fab was cleared from both tumor and surrounding brain rapidly because there was no antigen binding and no nonspecific binding to the Fc receptors present in the brain and tumor.

The tumor-specific L6 IgG not only has a prolonged plasma half-life and contains the Fc portion of the immunoglobulin but also has a high degree of antigen-specific binding. Delivery of L6 IgG to ICT showed good localization in nondisrupted animals and was only increased at early time points after BBBB. This may have an important effect when short half-life therapeutic isotopes or pharmaceuticals are used. In both nondisrupted and disrupted studies, L6 IgG persisted in tumor and normal brain for an extended period, probably as a result of the combination of a permeable brain tumor model, Mab specificity and nonspecific binding. The high level of antigen-specific binding resulted in the greater delivery and localization to both ICT and SQT compared with the control P1.17 IgG. Delivery of P1.17 IgG to the ICT demonstrates the effect of nonspecific binding, which showed significant nonspecific localization in nondisrupted animals, an increase after BBBB and a moderate rate of clearance between 24 and 72 hr after BBBB.

For unclear reasons, the P1.17 F(ab')₂ had an unusually long plasma half-life; L6 F(ab')₂ had an intermediate plasma half-life between that of Fab and intact IgG. F(ab')₂ fragments also lack the problem of nonspecific binding to Fc receptors. The results with the F(ab')₂ demonstrate minimal localization in nondisrupted animals and increased delivery after BBBB. However, localization did not persist. The explanation for this is thought to be, at least in part, more rapid dehalogenation of the F(ab')₂ compared with the intact IgG. Although L6 F(ab')₂ has an in vitro

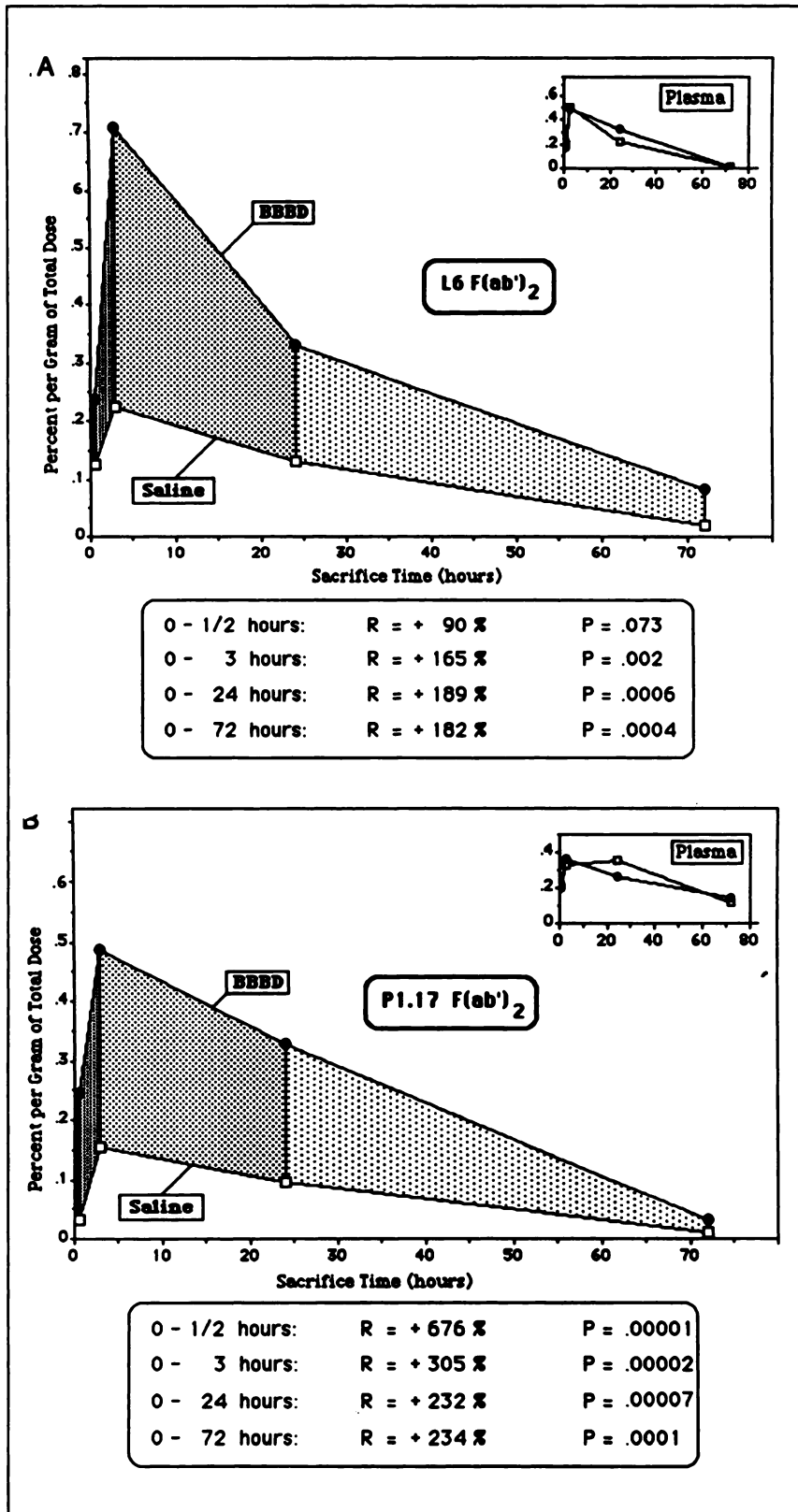


FIGURE 5. (A) Concentration (percent of total dose/g tissue) in intracranial tumor following intra-arterial administration of ^{125}I -labeled L6 F(ab')₂ after mannitol (BBBD) or saline as compared with intervals over time (0-72 hr). (B) Concentration (percent of total dose/g tissue) in intracranial tumor following intra-arterial administration of ^{125}I -labeled P1.17 F(ab')₂ after mannitol (BBBD) or saline as compared to intervals over time (0-72 hr). R = percent difference in the area under the curve for each integrated period.

antigen binding capacity that is similar to L6 IgG, an additional factor may be that the F(ab')₂ fragment antigen binding capacity is less stable in vivo.

CONCLUSION

The current studies showed increased Mab delivery with osmotic BBBD, most prominently with Fab and F(ab')₂. With or without BBBD, localization was greater for the specific Mab compared with the nonspecific Mab. These animal studies emphasize several factors aside from those that characterize systemic antibody pharmacokinetic properties (57) that collectively make it difficult to predict the outcome of future clinical Mab trials. Corticosteroids, used in most patients with brain tumors, are another variable that can effect Mab delivery (58). Clinical studies would most effectively determine which of these factors actually present problems in such patients. Such clinical trials would also provide direction for future animal studies.

REFERENCES

1. Bullard DE, Bigner DD. Applications of monoclonal antibodies in the diagnosis and treatment of primary brain tumors. *J Neurosurg* 1985;63:2-16.
2. Epenetos AA, Courtenay-Luck N, Pickering D, et al. Antibody-guided irradiation of brain glioma by arterial infusion of radioactive monoclonal antibody against epidermal growth factor receptor and blood group A antigen. *BMJ* 1985;290:1463-1466.
3. Zalutsky MR, Moseley RP, Coakham HB, et al. Pharmacokinetics and tumor localization of ¹³¹I-labeled anti-tenascin monoclonal antibody 81C6 in patients with gliomas and other intracranial malignancies. *Cancer Res* 1989;49:2807-2813.
4. Zalutsky MR, Moseley RP, Benjamin CJ, et al. Monoclonal antibody and F(ab')₂ fragment delivery to tumor in patients with glioma: comparison of intracarotid and intravenous administration. *Cancer Res* 1990;40:4105-4110.
5. Larson SM. Clinical radioimmunodetection 1978-1988: overview and suggestions for standardization of clinical trials. *Cancer Res* 1990;50:892-898.
6. Houghton AN, Mintzer D, Cordon-Cardo C, et al. Mouse monoclonal IgG3 antibody detecting GD₃ ganglioside: a phase I trial in patients with malignant melanoma. *Proc Natl Acad Sci USA* 1985;82:1242-1246.
7. Colston MJ, Fieldsteel AH, Dawson PJ. Growth and regression of human tumor cell lines in congenitally athymic (nu/nu) rats. *J Natl Cancer Inst* 1981;66:843-847.
8. Neuwelt EA, Frenkel E, D'Agostino AN, et al. Growth of human lung tumor in the brain of the nude rat as a model to evaluate antitumor agent delivery across the blood-brain barrier. *Cancer Res* 1985;45:2827-2833.
9. Wrobel CJ, Wright DC, Dedrick RL, et al. Diphtheria toxin effects on brain-tumor xenografts: implications for protein-based brain-tumor chemotherapy. *J Neurosurg* 1990;72:945-950.
10. Blasberg RG, Nakagawa H, Bourdon MA, et al. Regional localization of a glioma-associated antigen defined by monoclonal antibody 81C6 in vivo: kinetics and implications for diagnosis and therapy. *Cancer Res* 1987;47:4432-4443.
11. Bullard DE, Adams CJ, Coleman RE, et al. In vivo imaging of intracranial human glioma xenografts comparing specific with nonspecific radiolabeled monoclonal antibodies. *J Neurosurg* 1986;64:257-262.
12. Heisiger EM, Voorhies RM, Basler GA, et al. Opening the blood-brain and blood-tumor barriers in experimental rat brain tumors: the effect of intracarotid hyperosmolar mannitol on capillary permeability and blood flow. *Ann Neurol* 1986;19:50-59.
13. Neuwelt EA, Barnett PA. Blood-brain barrier disruption in the treatment of brain tumors: animal studies. In: Neuwelt EA, ed., *Implications of the blood-brain barrier and its manipulation: clinical aspects*. Vol. 2. New York: Plenum Press; 1989:107-194.
14. Rapoport SI. Osmotic opening of the blood-brain barrier. *Ann Neurol* 1988;24:677-684.
15. Robinson PJ. Facilitation of drug entry into brain by osmotic opening of the blood-brain barrier. *Clin Exp Pharmacol Physiol* 1987;14:887-901.
16. Robinson PJ, Rapoport SI. Size selectivity of blood-brain barrier permeability at various times after osmotic opening. *Am J Physiol* 1987;253:R459-R466.
17. Armstrong BK, Robinson PJ, Rapoport SI. Size-dependent blood-brain barrier opening demonstrated with [¹⁴C]sucrose and a 2,000,000-Da [³H]dextran. *Exp Neurol* 1987;97:686-696.
18. Ziyian YZ, Robinson PJ, Rapoport SI. Differential blood-brain barrier permeabilities to [¹⁴C]sucrose and [³H]inulin after osmotic opening in the rat. *Exp Neurol* 1983;79:845-857.
19. Neuwelt EA, Specht D, Larson S, et al. Increased delivery of tumor-specific monoclonal antibodies to brain after osmotic blood-brain barrier modification in patients with melanoma metastatic to the CNS. *Neurosurgery* 1987;20:885-895.
20. Lee Y-S, Bullard DE, Zalutsky MR, et al. Therapeutic efficacy of anti-glioma mesenchymal extracellular matrix ¹³¹I-radiolabeled murine monoclonal antibody in a human glioma xenograft model. *Cancer Res* 1988;48:559-566.
21. Neuwelt EA, Minna J, Frenkel E, et al. Osmotic blood-brain barrier opening to IgM monoclonal antibody in the rat. *Am J Physiol* 1986;250:R875-883.
22. Ovejera AA, Houchens DP. Human tumor xenografts in athymic nude mice as a preclinical screen for anticancer agents. *Semin Oncol* 1981;8:386-393.
23. Hellström I, Beaumier PL, Hellström KE. Antitumor effects of L6, and IgG_{2a} antibody that reacts with most human carcinomas. *Proc Natl Acad Sci USA* 1986;83:7059-7063.
24. Hellström I, Horn D, Linsley P, et al. Monoclonal mouse antibodies raised against human lung carcinoma. *Cancer Res* 1986;46:3917-3941.
25. Goodman GE, Hellström I, Brodzinsky L, et al. Phase I trial of murine monoclonal antibody L6 in breast, colon, ovarian, and lung cancer. *J Clin Oncol* 1990;8:1083-1092.
26. Nilaver G, Rosenbaum LC, Hellström I, et al. Identification of neurophysin immunoreactivity in human lung tumor and hypothalamus by a monoclonal antibody. *Neuroendocrinology* 1990;51:565-571.
27. Rosenbaum LR, Nilaver G, Loh YP, et al. Expression of neurophysin-related precursor in cell membranes of a small cell lung carcinoma. *Proc Natl Acad Sci USA* 1990;87:9928-9932.
28. Lamoyi E, Nisonoff A. Preparation of F(ab')₂ fragments from mouse IgG of various subclasses. *J Immunol Methods* 1983;56:235-243.
29. Beaumier PI, Neuzil D, Yang HM, et al. Immunoreactivity assay for labeled anti-melanoma monoclonal antibodies. *J Nucl Med* 1986;27:824-828.
30. Neuwelt EA, Barnett PA, Hellström KE, et al. Delivery of melanoma-associated immunoglobulin monoclonal antibody and Fab fragments to normal brain utilizing osmotic blood-brain barrier disruption. *Cancer Res* 1988;48:4725-4729.
31. Mardia KV, Kent JT, Bibby JM. *Multivariate analysis*. New York: Academic Press; 1979.
32. Fand I, Sharkey RM, Primus FJ, et al. Relationship of radioantibody localization and cell viability in a xenografted human cancer model as measured by whole-body autoradiography. *Cancer Res* 1987;47:177-2183.
33. Covell DG, Barbet J, Holton OD, et al. Pharmacokinetics of monoclonal immunoglobulin G₁, F(ab')₂, and Fab' in mice. *Cancer Res* 1986;46:3969-3978.
34. Blasberg RG, Groothuis D, Molnar P. A review of hyperosmotic blood-brain barrier disruption in seven experimental brain tumor models. In: Johansson BB, Owman C, Widner H, eds., *Pathophysiology of the blood-brain barrier*. Amsterdam: Elsevier Science Publishers; 1990.
35. Rapoport SI, Robinson PJ. A therapeutic role for osmotic opening of the blood-brain barrier. Re-evaluation of literature and of importance of source-sink relations between brain and tumor. In: Johansson BB, Owman C, Widner H, eds., *Pathophysiology of the blood-brain barrier*. Amsterdam: Elsevier Science Publishers, 1990:167-182.
36. Capone PM, Papsidero LD, Chu TM. Relationship between antigen density and immunotherapeutic response elicited by monoclonal antibodies against solid tumors. *J Natl Cancer Inst* 1984;72:673-677.
37. Carrasquillo JA, Krohn KA, Beaumier P, et al. Diagnosis of and therapy for solid tumors with radiolabeled antibodies and immune fragments. *Cancer Treat Rep* 1984;68:317-328.
38. Colapinto EV, Humphrey PA, Zalutsky MR, et al. Comparative localization of murine monoclonal antibody Mel-14 F(ab')₂ fragment and whole IgG_{2a} in human glioma xenografts. *Cancer Res* 1988;48:5701-5707.
39. de Tribolet N, Frank E, Mach J-P. Monoclonal antibodies: their application in the diagnosis and management of CNS tumors. In: Little JR, ed. *Clinical neurosurgery*. Baltimore: Williams & Wilkins; 1986:446-456.
40. Epenetos AA, Snook D, Durbin H, et al. Limitations of radiolabeled monoclonal antibodies for localization of human neoplasms. *Cancer Res* 1986;46:3183-3191.

41. Goldenberg DM. Current status of cancer imaging with radiolabeled antibodies. *J Cancer Res Clin Oncol* 1987;113:203-208.
42. Mayhan WG, Heistad DD. Permeability of blood-brain barrier to various sized molecules. *Am J Physiol* 1985;248:H712-H718.
43. Sharkey RM, Mabus J, Goldenberg DM. Factors influencing anti-antibody enhancement of tumor targeting with antibodies in hamsters with human colonic tumor xenografts. *Cancer Res* 1988;48:2005-2009.
44. Wahl RL, Liebert M, Wilson BS. The influence of monoclonal antibody dose on tumor uptake of radiolabeled antibody. *Cancer Drug Del* 1986;3:243-249.
45. Chamberlain MC, Murovic JA, Levin VA. Absence of contrast enhancement on CT brain scans of patients with supratentorial malignant gliomas. *Neurology* 1988;38:1371-1374.
46. Kelly PJ, Dumas-Duport C, Kispert DB. Imaging-based stereotaxic serial biopsies in untreated intracranial glial neoplasms. *J Neurosurg* 1987;66:865-874.
47. Kelly PJ, Dumas-Duport C, Scheithauer BW. Stereotactic histologic correlations of computed tomography- and magnetic imaging-defined abnormalities in patients with glial neoplasms. *Mayo Clin Proc* 1987;62:450-459.
48. Neuwelt EA, Dahlborg SA. Blood-brain barrier disruption in the treatment of brain tumors: clinical implications. In: Neuwelt EA, ed., *Implications of the blood-brain barrier and its manipulation: clinical aspects*. Vol. 2. New York: Plenum Press; 1989:195-262.
49. Lee Y-S, Bullard DE, Humphrey PA, et al. Treatment of intracranial human glioma xenografts with ¹³¹I-labeled antitenascin monoclonal antibody 81C6. *Cancer Res* 1988;48:2904-2910.
50. Hagan PL, Halpern SE, Dillman RO, et al. Tumor size: effect on monoclonal antibody uptake in tumor models. *J Nucl Med* 1986;27:422-427.
51. Colapinto EV, Zalutsky MR, Archer GE, et al. Radioimmunotherapy of intracerebral human glioma xenografts with ¹³¹I-labeled F(ab')₂ fragments of monoclonal antibody Mel-14. *Cancer Res* 1990;50:1822-1827.
52. Herlyn D, Powe J, Alavi A, et al. Radioimmunodetection of human tumor xenografts by monoclonal antibodies. *Cancer Res* 1983;43:2731-2735.
53. Wahl RL, Parker CW, Philpott GW. Improved radioimaging and tumor localization with monoclonal F(ab')₂. *J Nucl Med* 1983;24:316-325.
54. Zalutsky MR, Garg PK, Friedman HS, et al. Labeling monoclonal antibodies and F(ab')₂ fragments with the α -particle-emitting nuclide astatine-211: preservation of immunoreactivity in vivo localizing capacity. *Proc Natl Acad Sci USA* 1989;86:7149-7153.
55. Zalutsky MR, Noska MA, Colapinto EV, et al. Enhanced tumor localization and in vivo stability of a monoclonal antibody radioiodinated using N-succinimidyl 3-(tri-n-butylstanny)benzoate. *Cancer Res* 1989;49:5543-5549.
56. Bourdon MA, Coleman RE, Blasberg RG, et al. Monoclonal antibody localization in subcutaneous and intracranial human glioma xenografts: paired-label and imaging analysis. *Anticancer Res* 1984;4:133-140.
57. Bazter TB, Zhu H, Mackensen DG, et al. Physiologically based pharmacokinetic model for specific and nonspecific monoclonal antibodies and fragments in normal tissues and human tumor xenografts in nude mice. *Cancer Res* 1994;54:1517-1528.
58. Neuwelt EA, Barnett PA, Ramsey FL, et al. Dexamethasone decreases the delivery of tumor-specific monoclonal antibody to both intracerebral and subcutaneous tumor xenografts. *Neurosurgery* 1993;33:478-484.